Ab initio calculations on the $\tilde{X}\,^1A'$ and $\tilde{A}\,^1A''$ states of HPO and Franck-Condon simulation of the single vibronic level emission spectra of HPO and DPO

Edmond P. F. Lee,[a] Daniel K. W. Mok,[b),c)] and Foo-Tim Chau
Department of Applied Biology and Chemical Technology, The Hong Kong Polytechnic University, Hung Hom, Hong Kong

John M. Dyke[b),d)]
School of Chemistry, University of Southampton, Highfield, Southampton SO17 1BJ, United Kingdom

(Received 14 June 2007; accepted 6 September 2007; published online 6 December 2007)

Minimum-energy geometries and relative electronic energies of the $\tilde{X}\,^1A'$ and $\tilde{A}\,^1A''$ states of HPO have been computed employing the coupled-cluster single-double plus perturbative triple excitations {RCCSD(T)} and/or complete-active-space self-consistent-field (CASSCF) multireference internally contracted configuration interaction (MRCI) methods with basis sets of up to the augmented correlation-consistent polarized-valence quintuple-zeta (aug-cc-pV5Z) quality. In addition, RCCSD(T)/aug-cc-pVQZ and CASSCF/MRCI/aug-cc-pVQZ potential energy functions, anharmonic vibrational wave functions, and energies involving all three vibrational modes for both electronic states of HPO and DPO, and Franck-Condon factors between the two electronic states, which allow for Duschinsky rotation and anharmonicity, were computed. Computed Franck-Condon factors were then used to simulate single vibronic level (SVL) emission spectra recently reported by Tackett and Clouthier [J. Chem. Phys. **117**, 10604 (2002)]. Excellent agreement between the simulated and observed spectra was obtained for the $\tilde{A}\,^1A''(1,0,0)\rightarrow\tilde{X}\,^1A'$ SVL emission of HPO and DPO, when the best estimated *ab initio* geometries of the two states, which include contributions from core correlation and extrapolation to the complete basis set limit, were used in the simulation, suggesting that the best estimated *ab initio* geometry of the $\tilde{A}\,^1A''$ state of HPO, particularly the bond angle of 94.5°, is more reliable than the available experimentally derived geometry. A discussion on the geometrical parameters derived from rotational constants obtained from the rotational analysis of a high-resolution spectrum and from Franck-Condon simulation of the vibrational structure of an electronic spectrum is given. © *2007 American Institute of Physics*. [DOI: 10.1063/1.2790892]

I. INTRODUCTION

Recently, Tackett and Clouthier[1] reported the $\tilde{A}\,^1A''$-$\tilde{X}\,^1A'$ bands of HPO and DPO in laser induced fluorescence (LIF) and single vibronic level (SVL) emission spectra recorded from a jet-cooled pulsed electric discharge of a gas mixture of 15% H_2 or D_2 in 85% Ar over degassed phosphorous oxychloride ($POCl_3$). In this spectroscopic study,[1] by combining the rotational constants of DPO obtained from the rotational analysis of the high-resolution LIF 0_0^0 band of DPO and the rotational constants of HPO obtained from earlier emission spectrum of HPO,[2] equilibrium geometrical parameters of both the $\tilde{X}\,^1A'$ and $\tilde{A}\,^1A''$ states of HPO have been derived. As concluded by Tackett and Clouthier,[1] the most significant finding from their investigation is the decrease of the HPO bond angle from 104.62(7)° to 97.4(4)° upon excitation (for estimated equilibrium r_e^z structures, see Ref. 1). This decrease in the HPO bond angle is contrary to the prediction, according to Walsh's rules, of an increase in the bond angle of a 12 valence electron HAB system for an $n\rightarrow\pi^*$ (i.e., $\tilde{X}\,^1A'\rightarrow\tilde{A}\,^1A''$) excitation, as observed in HNO [an increase of the HNO bond angle of approximately 7° occurs from 108.6° to 116.3° (Ref. 3)] and other triatomic HAB systems (e.g., HSiF; see Ref. 1 and references therein). Nevertheless, such a decrease in the equilibrium HPO bond angle of approximately 7.2° as derived in Ref. 1 for the $\tilde{X}\,^1A'\rightarrow\tilde{A}\,^1A''$ excitation in HPO is in reasonably good agreement with a computed decrease of 6.1° (from 104.2° to 98.1°) obtained from quadratic configuration interaction single and double excitation (QCISD) calculations, also carried out in Ref. 1, on the $\tilde{X}\,^1A'$ and $\tilde{A}\,^1A''$ states of HPO using the augmented correlation-consistent polarized-valence triple-zeta (aug-cc-pVTZ) basis set. In fact, all available *ab initio* calculations on the $\tilde{X}\,^1A'$ and $\tilde{A}\,^1A''$ states of HPO suggest a decrease in the HPO bond angle upon excitation (see Ref. 1 and references therein). However, the magnitude of this decrease differs depending on the calculations carried out. For instance, when the two recent *ab initio* calculations on HPO carried out in Ref. 1 and 4 are considered, complete-active-space perturbation theory

[a)]Also at Southampton University. Electronic mail: epl@soton.ac.uk
[b)]Authors to whom correspondence should be addressed.
[c)]Electronic mail: bcdaniel@polyu.edu.hk
[d)]Electronic mail: jmdyke@soton.ac.uk

to the second-order (CASPT2) calculations performed by Luna *et al.*[4] (for earlier lower-level *ab initio* calculations carried out on HPO, see Ref. 4 and references therein) using the contracted [3*s*2*p*2*d*], [5*s*4*p*3*d*2*f*] and [6*s*5*p*4*d*3*f*] atomic natural orbital (ANO) basis sets for H, O, and P, respectively, gives a decrease in the HPO bond angle of 8.8° (from 104.1° to 95.3°) for the $\tilde{X}\,^1A' \rightarrow \tilde{A}\,^1A''$ excitation. This decrease is 2.7° larger than the corresponding QCISD value of Ref. 1 mentioned above. Since the bond angles of the $\tilde{X}\,^1A'$ state of HPO obtained from both *ab initio* calculations[1,4,5] and experimental sources[1,6] are very consistent (with a range within 1°; see Refs. 5 and 6, and also later text), the difference in the decrease in the HPO bond angle upon excitation between the CASPT2 and QCISD values originates essentially from the difference in the computed bond angles of the $\tilde{A}\,^1A''$ state of HPO. Specifically, the computed QCISD/aug-cc-pVTZ bond angle[1] is smaller than the CASPT2/ANO bond angle[4] for the $\tilde{A}\,^1A''$ state of HPO by 2.8°. Comparing these computed *ab initio* bond angles of the $\tilde{A}\,^1A''$ state of HPO with the experimentally derived value of 97.4° (r_e^z value) reported in the LIF study,[1] the latter value appears to agree better with the QCISD value of 98.1° than the CASPT2 value of 95.3°. However, the computed adiabatic electronic excitation energy (T_e) of 15 776 cm^{-1} for the $\tilde{A}\,^1A''$ state of HPO obtained from QCISD/aug-cc-pVTZ calculations of Ref. 1 agrees poorly with the experimental T_e value of 19 518.26 cm^{-1}.[1] Such a large difference of nearly 0.5 eV (over 3700 cm^{-1}) between the QCISD and experimental T_e values, which is almost certainly due to spin contamination in the unrestricted-spin Hartree-Fock wave function used for the low-spin open-shell singlet $\tilde{A}\,^1A''$ state in the QCISD calculations, casts doubt on the reliability of the computed geometry of the $\tilde{A}\,^1A''$ state of HPO obtained from the QCISD calculations. At the same time, although the computed CASPT2 T_e/T_0 values[4] of 17 243/16 823 cm^{-1} for the $\tilde{A}\,^1A''$ state of HPO agree much better than the QCISD values with the corresponding experimental values[1] of 19 518.26/19 032.778 cm^{-1}, the computed CASPT2 bond angle of 95.3° is smaller than the experimentally derived bond angle of 97.4° (r_e^z value[1]) by over 2°. Moreover, the discrepancies of over 0.28 eV (2275 cm^{-1}) between the CASPT2 and experimental T_e/T_0 values are still considerable and significantly larger than what would be expected from state-of-the-art *ab initio* calculations. In view of the above comparisons between theory and experiment on the T_e value and equilibrium geometrical parameters, particularly the bond angle, of the $\tilde{A}\,^1A''$ state of HPO, it is proposed to carry out state-of-the-art *ab initio* calculations on the $\tilde{X}\,^1A'$ and $\tilde{A}\,^1A''$ states of HPO in the present study, to hopefully reduce the discrepancies between theory and experiment.

It should also be noted that Franck-Condon (FC) simulation of the SVL emission spectra of HPO/DPO has also been carried out in Ref. 1, employing experimentally derived geometrical parameters for the two electronic states. The agreement between the simulated and observed spectra is reasonably good. However, the FC factors employed in the spectral simulations were calculated within the harmonic oscillator model (see Ref. 1 for details). In the present study, we also propose to perform FC factor calculations between the $\tilde{X}\,^1A'$ and $\tilde{A}\,^1A''$ states of HPO but to include anharmonicity, as it has been shown that anharmonicity can affect the quality of a simulated spectrum significantly.[7] Anharmonicity is also expected to be significant especially for a molecule, such as HPO, which contains a hydrogen atom, in the stretching mode involving H. Moreover, it is well known that FC factors are very sensitive to geometry changes in an electronic transition. In this connection, comparison between reliable simulated spectra, which include anharmonicity, and experimental spectra via the iterative Franck-Condon analysis[7,8] (IFCA) (*infra vide*) should yield reliable geometrical parameters of the upper state, if the geometry of the lower state is well established as in the case of the $\tilde{X}\,^1A'$ state of HPO.[1,5]

II. THEORETICAL CONSIDERATIONS AND COMPUTATIONAL DETAILS

A. Geometry optimization and relative electronic energy calculations

Geometry optimization calculations were carried out on the $\tilde{X}\,^1A'$ state of HPO employing both the coupled-cluster single and double[9] plus perturbative triple[10] excitations {CCSD(T)} and complete-active-space self-consistent-field[11] multireference internally contracted configuration interaction[12] (CASSCF/MRCI) methods. For the open-shell singlet $\tilde{A}\,^1A''$ state of HPO, only CASSCF/MRCI geometry optimization calculations were performed, and the computed MRCI energies including the Davidson correction (MRCI +D) were considered in the optimization in all cases. Three basis sets of different qualities were used to investigate the effects of basis set extension to the complete basis set (CBS) limit and core electron correlation on the computed quantities, namely, equilibrium geometrical parameters and relative electronic energies. When basis sets of aug-cc-pVQZ and aug-cc-pV5Z qualities[13] [the aug-cc-pV(Q+d)Z and aug-cc-pV(5+d)Z basis sets,[14] respectively, for the second row element P] were employed, core electrons were frozen in the RCCSD(T) and/or CASSCF/MRCI calculations. When the aug-cc-pCVQZ basis sets[15] were used for P and O, only the P $1s^2$ electrons were frozen in the correlation calculations. (We have also employed the aug-cc-pCVQZ basis set in valence only calculations; see later text.) The largest MRCI calculations carried out in the present study were on the $\tilde{X}\,^1A'$ state of HPO with the aug-cc-pCVQZ basis sets, which gave approximately 13.7×10^9 uncontracted configurations and approximately 28.8×10^6 internally contracted configurations.

Contributions of basis set extension to the CBS limit to the computed quantities were estimated[16] by taking half of the differences between the corresponding values obtained using the aug-cc-pV5Z and aug-cc-pVQZ basis sets (denoted CBS A in later text). In addition, we have also employed the two point extrapolation technique of the form $1/X^3$, designed for extrapolating correlation energies,[17] to estimate CBS contributions (denoted CBS B in later text). Contributions of core electron correlation to the computed quantities (denoted core A in later text) were estimated by taking the differences

of the corresponding values obtained using the aug-cc-pCVQZ basis set (including the P $2s^2 2p^6$ and O $1s^2$ electrons in the correlation calculations) and the aug-cc-pVQZ basis set (within the frozen core approximation). Also, core correlation has been estimated using computed quantities obtained from calculations using the aug-cc-pCVQZ basis set, with and without including core electrons (denoted core B in later text). The contributions of basis size extension to the CBS limit and core electron correlation to the optimized geometrical parameters and relative electronic energies have been assumed to be additive.

B. Potential energy functions, anharmonic vibrational functions, and Franck-Condon factors

Ab initio potential energy functions (PEFs) for the $\tilde{X}\,^1A'$ and $\tilde{A}\,^1A''$ states of HPO were obtained by fitting the following polynomial to calculated *ab initio* total electronic energies [CCSD(T) and MRCI+D energies, respectively],

$$V = \sum_{ijk} C_{ijk}(S_1)^i(S_2)^j(S_3)^k + V_{\mathrm{eqm}}. \quad (1)$$

The bending coordinate of Carter and Handy,[18] $S_2 = \Delta\theta + \alpha\Delta\theta^2 + \beta\Delta\theta^3$ has been employed for S_2, where $\Delta\theta$ is the displacement of the bond angle from the equilibrium value $(\theta - \theta_e)$, while S_1 and S_3 are the displacements of the HP and PO bond lengths from the equilibrium values $(r - r_e)$, respectively. 388 CCSD(T)/aug-cc-pVQZ energy points in the ranges of $0.88 \leqslant r(\mathrm{HP}) \leqslant 2.27$ Å, $54.3 \leqslant \theta(\mathrm{HPO}) \leqslant 155.15°$, and $1.18 \leqslant r(\mathrm{PO}) \leqslant 1.80$ Å were scanned for the $\tilde{X}\,^1A'$ state, and 206 CASSCF/MRCI/aug-cc-pVQZ energy points in the ranges of $0.82 \leqslant r(\mathrm{HP}) \leqslant 2.5$ Å, $35.6 \leqslant \theta(\mathrm{HPO}) \leqslant 158.0°$, and $1.15 \leqslant r(\mathrm{PO}) \leqslant 2.02$ Å were scanned for the $\tilde{A}\,^1A''$ state. All *ab initio* calculations reported in the present study were carried out using the MOLPRO suite of programs.[19]

The fitting of the PEFs, the variational calculations of the anharmonic vibrational wave functions, and the FC factor calculations performed have been described previously.[7,8] In brief, Watson's Hamiltonian[20,21] for a nonlinear molecule was used, and both anharmonicity and Duschinsky rotation were included in the FC factor calculations. Here, only some technical details specific to the present study are given. Anharmonic vibrational wave functions were expressed as linear combinations of harmonic oscillator functions, $h(v_1, v_2, v_3)$, where v_1, v_2, and v_3 denote the quantum numbers of the harmonic basis functions for the HP stretching, HPO bending, and PO stretching modes, respectively. Harmonic basis functions with vibrational quantum numbers up to $h(10, 15, 12)$ and a restriction of $v_1 + v_2 + v_3 \leqslant 15$ were included in the variation calculations of the $\tilde{X}\,^1A'$ state. For the $\tilde{A}\,^1A''$ state, harmonic basis functions up to $h(12, 12, 8)$, with a restriction of $v_1 + v_2 + v_3 \leqslant 12$, were considered. In the spectral simulation, vibrational components in the SVL $\tilde{X}\,^1A' \rightarrow \tilde{A}\,^1A''$ emission spectra of HPO/DPO were simulated using Gaussian functions with a full width at half maximum of 10 cm^{-1}. The relative intensity of each vibrational component in a simulated spectrum is given by the corresponding computed anharmonic FC factor and a frequency factor of power four.

IFCA carried out previously for other molecules held the geometry of the lower state involved in an electronic transition, usually the ground state, fixed to an available experimental equilibrium geometry. The geometrical parameters of the upper state were then varied systematically based on the computed *ab initio* geometry changes upon excitation/emission, until the best match between simulated and observed spectra was obtained (see Refs. 7 and 8 for details). In this way, equilibrium geometrical parameters of the upper state can be derived via IFCA. However, in the present study, it was found that employing the estimated best *ab initio* geometries of the two electronic states involved in the spectral simulation already yielded simulated spectra, which match very well with experimental spectra for both the HPO and DPO. Therefore, it appears that further IFCA is not required. This will be further discussed in the subsection on simulated spectra.

III. RESULTS AND DISCUSSION

The *ab initio* PEFs of the $\tilde{X}\,^1A'$ and $\tilde{A}\,^1A''$ states of HPO [C_{ijk} in Eq. (1) and β in the expression for S_2] obtained in the present study and the root-mean-square (rms) deviations of the fitted PEFs from the *ab initio* energy data points are given in Table I. The *ab initio* results are summarized in Tables II–V and some representative simulated spectra are compared with the observed spectra in Figs. 1 and 2. In the following subsections, the optimized geometrical parameters and computed vibrational frequencies of the $\tilde{X}\,^1A'$ state and the computed relative electronic energies of the $\tilde{A}\,^1A''$ state (T_e and T_0; with respect to the $\tilde{X}\,^1A'$ state) are discussed first because the comparison between theory and experiment for these quantities is relatively straightforward. Simulated and observed spectra will then be compared, followed by a discussion of the optimized geometrical parameters and computed vibrational frequencies of the $\tilde{A}\,^1A''$ state. Lastly, effective (r_0) geometrical parameters and rotational constants of the $\tilde{X}\,^1A'$ and $\tilde{A}\,^1A''$ states of HPO and DPO derived from different sources are discussed.

A. Optimized geometrical parameters of the $\tilde{X}\,^1A'$ state of HPO

For the $\tilde{X}\,^1A'$ state of HPO/DPO, the computed geometrical parameters and vibrational frequencies are summarized in Table II. Some available, published reliable theoretical and/or experimental values are also given for comparison (for lower-level or less reliable values, see Refs. 5 and 6). It can be seen that the equilibrium bond angles obtained from various sources as shown in Table II have very consistent values ranging between 104.1° and 104.6° as mentioned above, and hence no further discussion is required. For the equilibrium HP bond length, however, the CASSCF/MRCI values obtained with the three basis sets used in the present investigation are consistently smaller than the corresponding CCSD(T) values (with the same basis set used). The largest difference between the computed CCSD(T) and MRCI r_e(HP) is approximately 0.01 Å and is with the aug-cc-pCVQZ basis set (i.e., calculations which include core

TABLE I. The fitted RCCSD(T) and CASSCF/MRCI potential energy function (PEF) coefficients of the $\tilde{X}\,^1A'$ and $\tilde{A}\,^1A''$ states, respectively, of HPO obtained using the AVQZ basis set (see text).

$C(i,j,k)$[a]	$\tilde{X}\,^1A'$	$\tilde{A}\,^1A''$
200	0.3068	0.2778
020	1.0348	0.4973
002	0.1299	0.0521
110	0.0647	0.1115
101	−0.0174	0.0212
011	0.0845	0.0972
300	−0.5242	−0.5580
030	−2.1640	−1.1786
003	0.0201	−0.0609
210	0.0072	0.1519
201	0.0004	−0.0303
120	−0.0698	−0.1301
021	−0.0546	−0.1837
102	−0.0534	−0.0475
012	−0.1220	0.0644
111	−0.0797	−0.1362
400	0.6016	0.5777
040	2.8626	2.0737
004	0.0433	0.0899
310	−0.0474	0.0004
301	0.0100	0.0090
130	0.0165	−0.1051
031	−0.0486	−0.0820
103	−0.0210	0.0719
013	0.0199	0.0546
220	0.0922	0.0649
202	−0.0402	−0.0080
022	0.0043	0.0644
211	−0.0186	0.0423
121	0.1675	0.2049
112	0.1075	−0.0830
050	−3.3078	−2.2752
060	2.1692	0.9935
005	0.0592	−0.1421
006	0.0480	0.1082
500	−0.5390	−0.5937
600	0.2575	0.4094
β	−0.0780	−0.2571
rms[b] (cm^{-1})	1.5	5.5

[a]See text and Eq. (1) (subscripts 1, 2, and 3 correspond to the HP stretching, bending, and PO stretching modes, respectively).
[b]Root-mean-square deviations of the fitted PEFs from the *ab initio* energy data points.

correlation). For the equilibrium PO bond length, the computed CASSCF/MRCI values are larger than the corresponding CCSD(T) values by less than approximately 0.007 Å (with the same basis set used). Again, the largest difference is with the aug-cc-pCVQZ basis set. Effects of basis size extension to the CBS limit on the optimized geometrical parameters of the $\tilde{X}\,^1A'$ state of HPO are very small (less than 0.003 Å for bond lengths and 0.04° for the bond angle) with both the CASSCF/MRCI and CCSD(T) methods, and also with both extrapolation techniques (CBS corrections A and B in Table II), suggesting that the aug-cc-pVQZ basis set is reasonably adequate. However, although effects of core correlation on all three optimized geometrical parameters are small with the CCSD(T) method, its effect on the computed HP bond length with the CASSCF/MRCI method, a decrease of 0.011 Å, is not insignificant. In addition, basis set extension and core correlation contributions do not bring the best estimated MRCI geometrical parameters and the corresponding CCSD(T) values (best averaged values in Table II; see later text) significantly closer to each other. Since the CCSD(T) method is size consistent, but the MRCI method is not, the CCSD(T) results are therefore expected to be theoretically more reliable than the MRCI results.

Before comparing computed and experimental geometrical parameters of the $\tilde{X}\,^1A'$ state of HPO, it should be noted that the differences between the different ways of estimating core (cores A and B) and CBS (CBSs A and B) contributions mentioned above are very small (less than 0.0012 Å and 0.04° for bond lengths and angles, respectively). These differences are significantly smaller than estimated theoretical uncertainties associated with the estimated best theoretical values, which are the averaged values (best averaged values in Table II) of the core B+CBS A and core A+CBS B values (see Table II). These two combinations of core and CBS corrected values give the largest and smallest combined corrected values, respectively, thus giving the ranges of the estimated best theoretical values obtained, employing different core and CBS correction techniques. Comparison between computed and experimentally derived bond lengths indeed shows that the RCCSD(T) values give better agreement with the experimental values than the MRCI values, particularly for the PH bond length. It is pleasing to conclude that the estimated best CCSD(T) geometrical parameters of the $\tilde{X}\,^1A'$ state of HPO obtained in the present study agree with available experimentally derived r_e and r_e^z values from Refs. 6 and 1, respectively, to within 0.006 Å and 0.24°. The differences between the estimated best CCSD(T) and MRCI geometrical parameters, Δ{CCSD(T)-MRCI}, given in Table II for the $\tilde{X}\,^1A'$ state of HPO may be considered as reasonable estimates of the theoretical uncertainties associated with the computed CASSCF/MRCI geometrical parameters of the $\tilde{A}\,^1A''$ state of HPO, where the single reference CCSD(T) method is inadequate for the open-shell singlet excited state. It should also be noted that Δ{CCSD(T)-MRCI} for the bond angle of the $\tilde{X}\,^1A'$ state of HPO is only −0.11°, suggesting that the bond angle obtained using the MRCI method should be reasonably reliable.

Before the vibrational frequencies of the $\tilde{X}\,^1A'$ state of HPO are discussed, it should be mentioned that, when the present manuscript was in preparation, a very high level *ab initio* study on some XPO species, where X=H, F, Cl, and Br, has appeared.[22] In general, the computational strategies of this very recent study of Ref. 22 and the present study are very similar, though they differ in some details, which are described as follows. In Ref. 22, a series of cc-pV(n+d)Z basis sets, where n=T, Q, 5, and 6, were employed and the optimized geometrical parameters were extrapolated to the CBS limit using the functional forms of $1/n^3$ and $B\times\exp(-Cn)$ for the correlation and SCF levels, respectively (see Ref. 22 and references therein). In the present study, the augmented versions of the correlation-consistent basis sets,

TABLE II. Equilibrium geometrical parameters (r_e and θ_e in Å and deg, respectively) and vibrational frequencies (cm^{-1}) of the $\tilde{X}\,^1A'$ state of HPO (uncertainties in parentheses) obtained from different sources.

Method	r_e(HP)	r_e(PO)	θ_e(HPO)	ω_1(HP)	ω_2(bend)	ω_3(PO)
CAS/MRCI/VQZ	1.4537	1.4918	104.36			
CAS/MRCI/ACVQZ (frozen core)	1.4535	1.4907	104.38			
CAS/MRCI/ACVQZ	1.4424	1.4898	104.44			
CAS/MRCI/AV5Z	1.4534	1.4893	104.38			
CCSD(T)/AVQZ	1.4548	1.4873	104.33	2166.5	1008.0	1198.6
CCSD(T)/ACVQZ (frozen core)	1.4544	1.4861	104.37			
CCSD(T)/ACVQZ	1.4521	1.4829	104.34			
CCSD(T)/AV5Z	1.4546	1.4847	104.37			
CCSD(T)/AVQZ PEF; r_0, ν's	1.4730	1.4912	104.54	2066.9	983.4	1184.5
CCSD(T)/AVQZ PEF; r_e, ω's	1.4547	1.4873	104.32	2159.0	1003.9	1197.5
CCSD(T)/AVQZ PEF; DPO r_0, ν's	1.4680	1.4913	104.45	1508.7	737.8	1182.5
CCSD(T)/AVQZ PEF; DPO ω's				1552.6	748.8	1195.9
Est. MRCI core correction A[a]	−0.0113	−0.0020	+0.08			
Est. MRCI CBS correction A[b]	−0.0002	−0.0013	+0.01			
Est. MRCI CBS correction B[c]	−0.0003	−0.0026	+0.04			
MRCI (core A+CBS A) value[d]	1.4420(115)	1.4860(33)	104.47(9)			
MRCI (core A+CBS B) value[d]	1.4418(116)	1.4846(46)	104.50(12)			
Best averaged MRCI+D value[e]	1.442(12)	1.485(5)	104.49(12)			
Est. CCSD(T) core correction A[a]	−0.0027	−0.0044	+0.01			
Est. CCSD(T) core correction B[f]	−0.0023	−0.0032	−0.03			
Est. CCSD(T) CBS correction A[b]	−0.0001	−0.0013	+0.02			
Est. CCSD(T) CBS correction B[c]	−0.0002	−0.0026	+0.04			
CCSD(T) (core B+CBS A) value[d]	1.4522(24)	1.4802(45)	104.40(3)			
CCSD(T) (core A+CBS B) value[d]	1.4517(29)	1.4777(70)	104.36(1)			
Best averaged CCSD(T) value[e]	1.452(3)	1.479(7)	104.38(3)			
Δ {CCSD(T)-MRCI} values	+0.010	−0.006	−0.11			
Best theoretical r_0 of HPO[g]	1.470(3)	1.483(10)	104.60(8)			
Best theoretical r_0 of DPO[g]	1.465(3)	1.483(10)	104.51(8)			
QCISD/aug-cc-pVTZ[h]	1.457	1.494	104.2	2058[e]	1001[e]	1222[e]
CASPT2/ANO[i]	1.452	1.490	104.1	2096	977	1115
CCSD(T)/cc-pVTZ[5]	1.461	1.498	104.4	2140	1187	1005
CCSD(T)/AVQZ[5]	1.456	1.491	104.2			
CCSD(T)/cc-pV(Q+d)Z[j]	1.4551	1.4861	104.48	2163.7	1013.0	1202.6
CCSD(T)/cc-pV(5+d)Z[j]	1.4546	1.4843	104.41	2164.0	1006.9	1205.1
CCSD(T)/cc-pV(6+d)Z[j]	1.4544	1.4837	104.39			
CBS[j]	1.4541	1.4829	104.36			
CBS+CV[j]	1.4517	1.4791	104.34			
CBS+CV+SR[j]	1.4520(6)	1.4789(12)	104.33(5)			
LIF[l] HPO r_0, ν's	1.4772(13)	1.4843(2)	104.71(15)	2059(30)[k]	985(5)[k]	1188(5)
LIF[l] HPO r_e^z, ω's	1.4578(6)	1.480(1)	104.62(7)	2058(1)	1001(1)	1203(1)
LIF[l] DPO ν's				1502(30)[k]	741(5)[k]	1188(5)[k]
LIF[l] DPO ω's				1532(4)	752(2)	1209(2)
MW[6] r_0[l]	1.477	1.478	106.3			
MW[6] r_z[l]	1.473(7)	1.4843(9)	104.57(16)			
MW[6] r_e, ω's[l]	1.455(7)	1.4800(9)	[104.57][m]	2095(2)[n]	986(10)[n]	1188(10)[n]
Matrix IR[p] DPO				1530(20)[o]	750(10)[o]	1186(20)[o]

[a]The correction of core electron correlation contribution to the computed geometrical parameters takes the difference between the computed RCCSD(T) or MRCI values obtained using the AVQZ [frozen core RCCSD(T) or CASSCF/MRCI calculations] and the ACVQZ [frozen only the P $1s^2$ electrons in the RCCSD(T) or CASSCF/MRCI calculations] basis sets.

[b]The correction of extrapolation to the complete basis set (CBS) limit takes half of the difference between the values obtained using the AVQZ and AV5Z basis sets [at the RCCSD(T) or CASSCF/MRCI levels].

[c]The two-point extrapolation with the $1/X^3$ power form was used.

[d]The basis set extrapolation and core electron correlation contributions are assumed to be additive (to the AV5Z value). The theoretical uncertainties (in parentheses) are estimated by taking the differences between the corresponding core and CBS corrected CCSD(T) values and the CCSD(T)/AV5Z values. The two different combinations of core and CBS corrections give the largest and smallest combined values; see text.

[e]The average of the two different combined core and CBS corrected values.

[f]This core correlation correction has employed the aug-cc-pCVQZ basis set for both calculations with valence electron only and also including core electrons.
[g]The estimated best theoretical r_0 geometrical parameters have taken the corresponding best theoretical r_e values plus the differences between the r_0 and r_e geometrical parameters obtained from the RCCSD(T) PEF of the $\tilde{X}\,^1A'$ state of HPO. The uncertainty is estimated by the difference between the best theoretical value and the r_0 value obtained from the PEF.
[h]From Ref. 1; vibrational frequencies from B3LYP/aug-cc-pVQZ calculations.
[i]Contracted Gaussian atomic natural orbital (ANO) basis sets for H, O, and P: [3*s*2*p*1*d*], [5*s*4*p*3*d*2*f*], and [6*s*5*p*4*d*3*f*], respectively; see original work of Luna *et al.* (Ref. 4).
[j]See text and Ref. 22.
[k]The estimated uncertainties used in the force field refinement carried out in Ref. 1 are given in parentheses.
[l]Experimental vibrational frequencies from previous works (see Ref. 6 and reference therein).
[m]Assumed to be equal to θ_z; see original work of Ref. 6.
[n]Estimated errors due to matrix shift and anharmonicity (see Refs. 6 and 24).
[o]Estimated errors due to anharmonicity; see Refs. 2 and 6.
[p]Reference 24.

which include sets of diffuse functions, aug-cc-pV(n+d)Z, where n=Q and 5, have been used with a simple CBS correction, as described above. For core [or core valence (CV in Table II) as used in Ref. 22] correlation contributions to the optimized geometrical parameters, the energy-weighed cc-pwCVQZ basis set was used in Ref. 22, while the aug-cc-pCVQZ basis set was used in the present study. Scalar relativistic (SR in Table II) contributions to optimized geometrical parameters were computed explicitly in Ref. 22, but were concluded to be essentially negligible, thus justifying the neglect of scalar relativistic contributions in the present study. Comparison between the cc-pV(5+d)Z and AV5Z results obtained from Ref. 22 and the present study, respectively, shows that the differences in the optimized geometrical parameters are negligibly small (less than 0.0005 Å and 0.04° in bond lengths and angle, respectively). However, the differences between the cc-pV(Q+d)Z and AVQZ geometrical parameters are significantly larger and of the order of 0.001 Å and 0.15°, suggesting that with the relatively smaller quadruple-zeta (QZ) quality basis sets, the effects of diffuse functions in the augmented part of the basis sets on the equilibrium geometrical parameters are not negligible. The more significant differences between with and without augmented diffuse functions in the basis sets are the directions of changes in the optimized geometrical parameters (i.e. an increase or a decrease; particularly for the bond angle) from employing the QZ to 5Z quality basis sets, which determine the directions of the extrapolation to the CBS limit. Specifically, without the augmented diffuse functions [i.e. with the cc-pV(Q+d)Z and cc-pV(5+d)Z basis sets in Ref. 22], the computed equilibrium bond angle decreases with the improvement of basis sets. However, with the augmented diffuse functions (i.e. with the AVQZ and AV5Z basis sets in the present study), it increases. Nevertheless, both the increase and decrease are small [0.02° and 0.07° (from QZ to 5Z), respectively], and it is pleasing that the estimated best theoretical geometrical parameters of the $\tilde{X}\,^1A'$ state of HPO obtained here agree with those of Ref. 22 (CBS+CV and/or CBS+CV+SR values in Table II) to within 0.0003 Å and 0.05°, showing that these best theoretical estimates are very consistent and hence can be concluded to be highly reliable.

B. Computed vibrational frequencies of the $\tilde{X}\,^1A'$ state of HPO

It is pleasing that the computed fundamental frequencies of all three vibrational modes of the $\tilde{X}\,^1A'$ state of both HPO and DPO obtained from the CCSD(T)/aug-cc-pVQZ PEF of the present work agree very well with the corresponding experimental values (to within 7 cm^{-1}; Table II). For the harmonic frequencies, the computed HPO bending and PO stretching values also agree reasonably well with the experimentally derived values for both HPO and DPO. However, for the PH and PD stretching modes, the computed harmonic frequencies obtained from the CCSD(T)/aug-cc-pVQZ PEF are significantly larger than the corresponding experimentally derived values for both HPO and DPO. It should be noted that estimated uncertainties of 30 cm^{-1} were given in Ref. 1 for the harmonic HP and DP stretching frequencies used in the force field refinement (see footnote *g* of Table II and the original reference). Such estimated uncertainties, which are rather large, are due to limitations in the range of experimental data (e.g. in the emission spectrum, 1_1^0 is observed, but 1_2^0 is not observed). In Ref. 1, the experimentally measured fundamental frequencies of the HP and DP stretching modes of HPO and DPO given are smaller than the corresponding experimentally derived harmonic frequencies by only −1 and 30 cm^{-1}, respectively. These small differences, particularly for the HP stretching mode, suggest very small anharmonicities, which are contrary to expectation for these vibrational modes. In view of the above considerations, it is concluded that the computed harmonic HP/DP frequencies reported here (which are higher than those quoted in Ref. 1 by 101 and 20 cm^{-1}, respectively) are almost certainly more reliable than the experimentally derived values from Ref. 1, as the HP (DP) stretching mode is expected to be significantly anharmonic. The computed harmonic HP stretching frequencies obtained with the cc-pV(Q+d)Z and cc-pV(5+d)Z basis sets from Ref. 22 also agree very well with our computed AVQZ values (from both numerical second derivative calculations and the PEF) and are larger than the experimentally derived harmonic values by more than 100 cm^{-1}, reinforcing the conclusion that the theoretical harmonic values obtained here and in Ref. 22 are more reliable than the experimentally derived values (Ref. 1).

TABLE III. Computed relative electronic energies, T_e (in eV/cm^{-1}), of the $\tilde{A}\,^1A''$ state of HPO with respect to the $\tilde{X}\,^1A'$ state.

Methods	T_e
CAS/AVQZ[a]	3.1415/25 660
CAS/MRCI/AVQZ[a]	2.5437/20 516
CAS/MRCI+D/AVQZ[a]	2.4218/9 533
CAS/ACVQZ (frozen core)[b]	3.1908/25 735
CAS/MRCI/ACVQZ (frozen core)[b]	2.5483/20 554
CAS/MRCI+D/ACVQZ (frozen core)[b]	2.4255/19 563
CAS/AV5Z[c]	3.1929/25 752
CAS/MRCI/AV5Z[c]	2.5593/20 642
CAS/MRCI+D/AV5Z[c]	2.4367/19 653
CAS/ACVQZ[d]	3.1951/25 770
CAS/MRCI/ACVQZ[d]	2.5100/20 244
CAS/MRCI+D/ACVQZ[d]	2.3600/19 035
Estimated core correction A[e]	−0.0617/−498
Estimated core correction B[f]	−0.0655/−528
Estimated CBS correction A[g]	+0.0074/+60
Estimated CBS correction B[h]	+0.0156/+126
(core B+CBS A) T_e[i]	2.3786±0.0581/19 185±468
(core A+CBS B) T_e[i]	2.3906±0.0461/19 281±372
Best averaged T_e[j]	2.38±0.06/19 233±470
ΔZPE correction (HPO)[k]	−0.0596/−480.4
Best theoretical T_0 (HPO)	2.33±0.06/18 753±480
ΔZPE correction (DPO)[l]	−0.0538/−434.2
Best theoretical T_0 (DPO)	2.33±0.06/18 799±475
QCISD/aug-cc-pVTZ[l]	1.9560/15 776
CASPT2/ANO[l] T_e	2.1379/17 243
CASPTS/ANO[l] T_0	2.0858/16 823
Emission[2] T_0 (HPO)	2.3598/19 032.778(7)
LIF/emission[l] T_0 (HPO)	2.3598/19 032.778
LIF/emission[l] T_0 (DPO)	2.3682/19 100.901
LIF/emission[l] T_e (HPO)	2.4200(3)/19 518.26(280)
LIF/emission[l] T_e (DPO)	2.4231(6)/19 543.60(448)

[a]At corresponding CASSCF/MRCI/AVQZ geometries.
[b]At corresponding CASSCF/MRCI/ACVQZ (frozen core) geometries.
[c]At corresponding CASSCF/MRCI/AV5Z geometries.
[d]At corresponding CASSCF/MRCI/ACVQZ geometries.
[e]The correction of core electron correlation contribution takes the difference between the values obtained using the AVQZ (frozen core CASSCF/MRCI+D calculation) and the ACVQZ (frozen only the P $1s^2$ electrons in the CASSCF/MRCI+D calculation) basis sets.
[f]This core correlation correction has employed the aug-cc-pCVQZ basis set for both calculations with valence electrons only and also including core electrons.
[g]The correction of extrapolation to the complete basis set (CBS) limit takes half of the difference between the values obtained using the AVQZ and AV5Z basis sets.
[h]The two-point extrapolation with the $1/X^3$ power form was used.
[i]Assuming that the basis set extrapolation and core electron correlation contributions are additive (to the CASSCF/MRCI+D/AV5Z value). The theoretical uncertainties (in parentheses) are estimated by taking the differences between the best estimated values and the MRCI+D/AV5Z values. The two different combinations of core and CBS corrections give the smallest and largest combined values.
[j]The average of the two different combined core and CBS corrected values.
[k]Using experimental fundamental vibrational frequencies from Ref. 1.
[l]CASPT2 T_e and T_0 values are 49.3 and 48.1 kcal/mole (17 243 and 16 823 cm^{-1}), respectively; see original work of Luna *et al.* (Ref. 4).

C. Relative electronic energies: T_e and T_0 of the $\tilde{A}\,^1A''$ state

The computed T_e and T_0 values of the $\tilde{A}\,^1A''$ state of HPO are compared with available theoretical and experimental values in Table III. It can be seen from the computed results obtained from the present study that dynamic electron correlation is very important for the reliability of computed relative electronic energies. Specifically, the computed CASSCF T_e values, which are larger than the MRCI values (without the Davidson correction) by over 0.6 eV, are clearly inadequate. In addition, the Davidson correction further reduces the calculated T_e values obtained at the MRCI level by approximately 0.12 eV with the aug-cc-pVQZ and aug-cc-pV5Z basis sets and by 0.15 eV with the aug-cc-pCVQZ basis set (including core correlation), indicating that contributions from the Davidson correction to computed relative electronic energies are significant. Estimated CBS and core correlation corrections to the computed T_e value are therefore evaluated only employing the MRCI+D values. The CBS corrections obtained by the two methods employed, of less than +0.016 eV, are relatively small, but the core correlation corrections obtained by the two methods employed of approximately −0.066 eV are considerable. The largest and smallest combined core and CBS corrected values employing different methods are 2.379 and 2.391 eV, respectively (Table III). The estimated best theoretical T_e value is 2.38±0.06 eV (best averaged T_e in Table II). It is pleasing that the discrepancy of less than 0.04 eV between this estimated best *ab initio* T_e and the available experimental value of approximately 2.42 eV (for HPO/DPO from Ref. 1; see Table III) is within the estimated theoretical uncertainty of approximately ±0.06 eV. The T_0 value of the $\tilde{A}\,^1A''$ state of HPO and DPO has also been evaluated based on the estimated best *ab initio* T_e value, employing experimental fundamental vibrational frequencies of Ref. 1 for zero-point energy corrections (ΔZPE). The estimated best *ab initio* T_0 values of 2.33 eV (18 753 cm^{-1}) and 2.33 eV (18 799 cm^{-1}) agree very well with available experimental values of 2.3598 eV (19 032.778 cm^{-1})[1,2] and 2.3682 eV (19 100.901 cm^{-1}) (Ref. 1) for HPO and DPO, respectively.

It is noted that the computed CASSCF/MRCI+D T_e values of 2.42 and 2.44 eV, obtained using the aug-cc-pVQZ and aug-cc-pV5Z basis sets, respectively (Table III), actually agree almost exactly with the experimental value of 2.42 eV. However, this excellent agreement between theory and experiment is almost certainly fortuitous and is due to cancellation of errors arising from the neglect of core correlation and the lack of size consistency of the MRCI method. Nevertheless, the above comparison suggests that the CASSCF/MRCI+D/aug-cc-pVQZ level of calculation should be reasonably adequate for the $\tilde{A}\,^1A''$ state of HPO.

Summarizing, state-of-the-art *ab initio* calculations carried out in the present investigation give T_e/T_0 values for the $\tilde{A}\,^1A''$ state of HPO/DPO, which agree with available experimental values to within approximately 0.04 eV (approximately 320 cm^{-1}). This good agreement between theory and experiment demonstrates clearly that the *ab initio* calculations carried out in the present study are superior to previous calculations (such as those in Refs. 1 and 4), and that state-of-the-art *ab initio* calculations are able to give very reliable relative electronic energies. This increases our confidence in the reliability of the geometrical parameters of the $\tilde{A}\,^1A''$ state of HPO obtained in the present study.

TABLE IV. Optimized geometrical parameters (r_e and θ_e in Å and deg, respectively) and computed vibrational frequencies of the $\tilde{A}\,^1A''$ state of HPO (cm^{-1}, uncertainties in parentheses).

Methods	r_e(HP)	r_e(PO)	θ_e(HPO)	ω_1(HP)	ω_2(bend)	ω_2(PO)
MRCI/AVQZ	1.4529	1.5815	94.00			
MRCI/ACVQZ (frozen core)	1.4527	1.5800	94.06			
MRCI/ACVQZ	1.4484	1.5741	94.20			
MRCI/AV5Z	1.4532	1.5771	94.21			
MRCI/AVQZ PEF; r_0, ν's	1.4735	1.5798	95.08	1858.4	560.9	831.9
MRCI/AVQZ PEF; r_e, ω's	1.4530	1.5810	94.09	2054.7	596.2	834.4
MRCI/AVQZ PEF; DPO r_0, ν's	1.4677	1.5821	94.77	1380.5	432.7	808.5
MRCI/AVQZ PEF; DPO ω's				1478.0	450.1	816.7
Est. core correction A[a]	−0.0045	−0.0074	+0.20			
Est. core correction B[b]	−0.0043	−0.0059	+0.14			
Est. CBS correction A[c]	+0.0002	−0.0022	+0.11			
Est. CBS correction B[d]	+0.0003	−0.0045	+0.22			
(core B+CBS A) values[e]	1.4491(41)	1.5690(81)	94.46(25)			
(core A+CBS B) values[e]	1.4490(42)	1.5652(119)	94.63(42)			
Best averaged MRCI+D values[f]	1.449(4)	1.567(12)	94.5(4)			
Best theoretical r_0 of HPO[g]	1.470(4)	1.566(14)	95.4(4)			
Best theoretical r_0 of DPO[g]	1.464(4)	1.567(14)	95.1(4)			
QCISD/aug-cc-pVTZ[h]	1.428	1.577	98.1	2116[h]	513[h]	960[h]
CASPT2/ANO[i]	1.450	1.573	95.3	1971	521	896
LIF r_0, ν's	1.4920(2)	1.5612(1)	97.69(3)	1849(30)[j]	566(5)[j]	858(5)[j]
LIF r_c^z, ω's	1.4671(26)	1.5579(6)	97.4(4)	1848(1)	564(2)	871(1)
LIF; DPO ν's				1294(30)[j]	431(5)[j]	836(5)[j]
LIF; DPO ω's				1303(2)	435(2)	859(2)

[a]The correction of core electron correlation contribution takes the difference between the values obtained using the AVQZ (frozen core CASSCF/MRCI+D calculation) and the ACVQZ (frozen only the P $1s^2$ electrons in the CASSCF/MRCI+D calculation) basis sets.
[b]This core correlation correction has employed the aug-cc-pCVQZ basis set for both calculations with valence electrons only and also including core electrons.
[c]The correction of extrapolation to the complete basis set (CBS) limit takes half of the difference between the values obtained using the AVQZ and AV5Z basis sets.
[d]The two-point extrapolation with the $1/X^3$ power form was used.
[e]Assuming that the basis set extrapolation and core electron correlation contributions are additive (to the CASSCF/MRCI+D/AV5Z value). The theoretical uncertainties (in parentheses) are estimated by taking the differences between the best estimated values and the MRCI+D/AV5Z values. The two different combinations of core and CBS corrections give the largest and smallest combined values.
[f]The average of the two different combined core and CBS corrected values.
[g]The estimated best theoretical r_0 geometrical parameters have taken the corresponding best theoretical r_e values plus the differences between the r_0 and r_e geometrical parameters obtained from the CASSCF/MRCI PEF of the $\tilde{X}\,^1A'$ state of HPO. The uncertainty is estimated by the difference between the best theoretical value and the r_0 value obtained from the PEF.
[h]From Ref. 1; vibrational frequencies from B3LYP/aug-ccVQZ calculations.
[i]From Ref. 4.
[j]The estimated uncertainties of the fundamental vibrational frequencies used in the force field refinement carried out in Ref. 1 are given in parentheses. The large uncertainty of 30 cm^{-1} associated with ν_1 is to account for the expectedly large, but uncertain, anharmonicity for the PH stretching mode (see text and original work).

D. Simulated spectra

Some representative simulated spectra (middle and bottom traces) are compared with the experimental $\tilde{A}\,^1A''(0,0,0)-\tilde{X}\,^1A'$ SVL emission spectra of HPO and DPO from Ref. 1 (top traces) in Figs. 1 and 2, respectively. The *ab initio* PEFs and the associated sets of geometrical parameters for the two states involved have been used to obtain the simulated spectra. The simulated spectra shown in the middle and bottom traces of each figure have employed available experimental r_e^z geometries from Ref. 1, and the best *ab initio* equilibrium geometries estimated in the present study, respectively, for both electronic states. Firstly, the overall general agreement between the simulated and observed spectra is very good, thus confirming the molecular carrier of, electronic states involved in, and the vibrational assignments of the experimental SVL emission spectra given in Ref. 1.

Secondly, it can be seen from Figs. 1 and 2 that the simulated spectra of both HPO and DPO obtained employing the best *ab initio* geometries of the two states (bottom traces) match the observed spectra better than those obtained employing the experimentally derived geometries of the two states (middle traces). The most obvious indication lies in the relative intensities of the relatively strong 2_1^0 and 3_1^0 vibrational components. Specifically, the relative intensities of the 2_1^0 components in simulated spectra of both the HPO and DPO obtained employing the experimental geometries are too weak, when compared with the observed spectra. In ad-

TABLE V. Summary of various effective r_0 geometries and the corresponding rotational constants (when no geometrical parameters are given, the A_0, B_0, and C_0 values are derived from high-resolution spectroscopic data; see original work) (A_0, B_0, and C_0 in cm^{-1}) of the $\tilde{X}\,^1A'$ and $\tilde{A}\,^1A''$ states of HPO and DPO (the values of atomic mass used for D, P, and O in the evaluation of the rotational constants of DPO from the specified geometrical parameters are 2.014 101 779, 30.973 762 0, and 15.994 914 63, respectively) obtained from different methods (uncertainties in parentheses).

Methods	r_0(HP)	r_0(PO)	θ_0	A_0	B_0	C_0
HPO $\tilde{X}\,^1A'$						
CCSD(T)/AVQZ PEF	1.4730	1.4912	104.54	8.701	0.694	0.642
Best RCCSD(T)[a]	1.4703	1.4829	104.60	8.740(39)	0.702(8)	0.650(8)
Emission[b]				8.851 1(18)	0.703 43(44)	0.649 75(44)
MW[c]				8.838 37(46)	0.703 014(1)	0.649 221(1)
MW r_0[c]	1.477	1.487	106.3	8.836	0.704	0.652
LIF r_0[d]	1.4772	1.4843	104.71	8.670	0.700	0.648
DPO $\tilde{X}\,^1A'$						
CCSD(T)/AVQZ PEF	1.4680	1.4913	104.45	4.641	0.677	0.591
Best theoretical[a]	1.4653	1.4830	104.51	4.663(22)	0.676(1)	0.590(1)
MW[c]				4.708 38(23)	0.677 412(1)	0.590 035(1)
LIF[d]				4.707 8(14)	0.677 11(36)	0.589 56(35)
HPO $\tilde{A}\,^1A''$						
MRCI/AVQZ PEF r_0	1.4735	1.5798	95.08	8.075	0.629	0.583
Best theoretical r_0[a]	1.4695	1.5658	95.44	8.134(59)	0.640(11)	0.593(10)
Emission[b]				8.268 9(9)	0.643 07(5)	0.593 68(5)
Emission r_0[b]	1.51	1.549	105	8.318	0.643	0.597
LIF r_0[d]	1.4920	1.5612	97.69	7.990	0.641	0.594
DPO $\tilde{A}\,^1A''$						
MRCI/AVQZ PEF	1.4677	1.5821	94.77	4.234	0.615	0.537
Best theoretical[a]	1.4637	1.5669	95.13	4.275(41)	0.627(12)	0.547(10)
LIF[d]				4.318 6(10)	0.628 46(10)	0.544 76(38)

[a]The estimated best theoretical r_0 geometrical parameters have taken the corresponding best theoretical r_e values plus the differences between the r_0 and r_e geometrical parameters obtained from the RCCSD(T) or CASSCF/MRCI PEF of the $\tilde{X}\,^1A'$ or $\tilde{A}\,^1A''$ state of HPO. The uncertainties of the rotational constants obtained from the best theoretical r_0 geometrical parameters (in parentheses) are estimated by taking the differences between the r_0 rotational constants obtained from the PEF and those obtained with the best theoretical r_0 geometry.
[b]Reference 2.
[c]Reference 6.
[d]Reference 1.

dition, observed weaker vibrational structure also matches better the simulated spectra obtained using the best *ab initio* geometries than using the experimental geometries. For instance, the observed shape of the relatively weak 2_2^0 and 1_1^0 vibrational overlapping components at 1468.9 and 1501.9 cm^{-1} in the experimental spectrum [experimental redshift energy from Ref. 1 (corresponding computed redshift energies: 1466.6 and 1508.7 cm^{-1}); labeled 2_2^0 in Fig. 2 top trace] in the $\tilde{A}\,^1A''(0,0,0)-\tilde{X}\,^1A'$ SVL emission spectrum of DPO matches the computed relative intensities using the best *ab initio* geometries (bottom trace in Fig. 2) better than the relative intensities using the experimental geometries (middle trace in Fig. 2).

Thirdly, it should also be noted that the emission spectra recorded using a photomultiplier in Ref. 1 have not been corrected for wavelength dependence of detector sensitivity, as stated therein. With the type of detector used in Ref. 1, it is anticipated that detector sensitivity would decrease toward low emission energy (see, for example, Ref. 23). Taking this experimental factor into consideration, the simulated spectra obtained using the best *ab initio* geometries would match even better the observed spectra if the experimental spectra were corrected for wavelength dependent detector sensitivity.

Lastly, further IFCA using different geometrical parameters for either or both states of HPO in order to obtain better matches between simulated and observed spectra has not been carried out. This is, of course, mainly because the simulated spectra obtained using the best *ab initio* geometries of both states already match the observed spectra very well, as discussed. In addition, although the changes in the equilibrium PO bond length and HPO bond angle upon emission obtained from the best *ab initio* estimation in the present study and those derived from the spectroscopic study of Ref. 1 are in the same directions (i.e., PO decreases and θ increases), the changes in the equilibrium HP bond length upon emission obtained from these two sources are in opposite directions. Specifically, *ab initio* calculations give a small increase in the HP bond length (0.003 Å) upon emission, while the experimentally derived geometries give a small decrease (0.0094 Å). Unfortunately, comparison between simulated and observed spectra provides information only on the magnitudes of the changes in the geometrical parameters

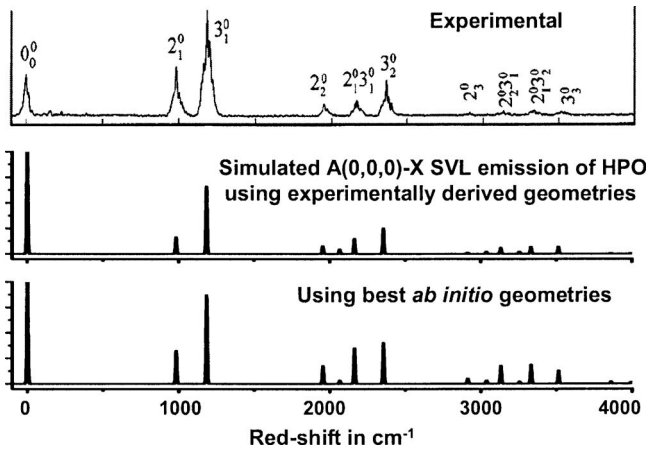

FIG. 1. Comparison between experimental (top; from Ref. 1) and simulated $\tilde{A}\,^1A''(0,0,0)-\tilde{X}\,^1A'$ SVL emission spectra of HPO, employing the experimentally derived (middle) and best *ab initio* (bottom) geometries of the two states (see text for details).

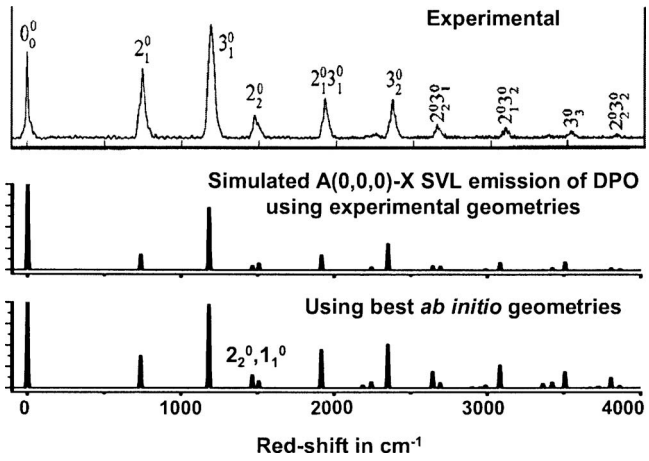

FIG. 2. Comparison between experimental (top; from Ref. 1) and simulated $\tilde{A}\,^1A''(0,0,0)-\tilde{X}\,^1A'$ SVL emission spectra of DPO, employing the experimentally derived (middle) and best *ab initio* (bottom) geometries of the two states (see text for details).

used in the simulation, but is unable to inform us on the direction of the changes. At present, it is uncertain which direction of change in the HP bond length upon emission is more reliable. Nevertheless, the increase and decrease in the HP bond length upon emission obtained from the present study and Ref. 1, respectively, can be considered as relatively small. The geometry of the $\tilde{A}\,^1A''$ state of HPO, particularly the bond angle, will be further discussed in the next subsection. It is concluded here that comparison between simulated and observed SVL emission spectra of HPO and DPO indicates that the geometry change upon emission based on best *ab initio* geometries of both states is highly reliable.

E. Optimized geometrical parameters and computed vibrational frequencies of the $\tilde{A}\,^1A''$ state of HPO

Ab initio results are summarized and compared with available computed and experimental values in Table IV. Firstly, computed equilibrium bond lengths and bond angles of the $\tilde{A}\,^1A''$ state of HPO obtained at different levels of calculation in the present investigation have very consistent values. It can be seen from Table IV that basis set extension effects on the computed geometrical parameters are very small (smaller than 0.005 Å and 0.22°). Core correlation effects are slightly larger (approximately 0.007 Å and 0.20°), but still can be considered as relatively small. One most important finding is the consistency in the computed bond angles obtained in the present study. Specifically, the spread of the computed values obtained using three basis sets is only 0.21° and the estimated best *ab initio* value of 94.5° (best averaged MRCI+D value in Table IV) has an estimated uncertainty of ±0.4°. The best *ab initio* value obtained here agrees reasonably well with the CASPT2 value of 95.3° from Ref. 4, but is smaller than the QCISD value of 98.1 and the experimentally derived r_c^z value of 97.4° from Ref. 1 by over 2°. Based on results of state-of-the-art *ab initio* calculations and spectral simulations obtained in the present study, it is concluded that the estimated best *ab initio* bond angle of 94.5° is most likely, currently, the most reliable value. We will further discuss experimentally derived rotational constants and r_0 structures of HPO and DPO in the next subsection.

The computed harmonic and fundamental vibrational frequencies of the $\tilde{A}\,^1A''$ state of HPO and DPO obtained from the MRCI PEF in the present study are given in Table IV. The computed fundamental frequencies of the HP stretching mode and bending mode of HPO and the bending mode of DPO agree very well with the corresponding experimental values measured from the LIF spectra of Ref. 1. The discrepancies between theory and experiment for these vibrational modes are less than 10 cm^{-1}. For the PO stretching modes of HPO and DPO, the computed fundamental frequencies are smaller than the corresponding measured values by approximately 28 cm^{-1}. This difference between theory and experiment may still be considered as reasonably small. However, the difference between the computed and experimental fundamental frequency of the DP stretching mode of DPO is 86.5 cm^{-1}. It is not immediately clear what is the cause of such a large discrepancy between theory and experiment for this vibrational mode, as the agreement between the computed and measured fundamental frequencies of the HP mode is very good (within approximately 9 cm^{-1}), and the same PEF has been used to calculate the fundamental frequencies of both the HP and DP stretching modes of HPO and DPO, respectively. It should, however, be noted that $3v_2'$ (3×431 cm^{-1}) of DPO is expected to have a value of approximately 1293 cm^{-1}, which would make it almost coincide with the observed band assigned to 1_0^1 (1293.799 cm^{-1} redshift energy from Table 1 of Ref. 1; see also Table IV) in the LIF spectrum of DPO. In this connection, we speculate that the assignment of the observed band assigned previously to 1_0^1 may actually be 2_0^3. Assuming that the computed fundamental frequency of the DP stretching mode of the $\tilde{A}\,^1A''$ state of DPO obtained here is reliable, the 1_0^1 band is expected to be at approximately 20 481 cm^{-1} excitation energy in the LIF spectrum of DPO. However, based on the data and discussion given in Ref. 1, no spectral band seems to be identifiable in this region of the LIF spectrum of DPO. Further investigation is required to firmly determine the DP stretching frequency of DPO.

F. Effective (r_0) geometrical parameters and rotational constants

The effective (r_0) geometrical parameters and rotational constants (i.e., A_0, B_0, and C_0) of the $\tilde{X}\,^1A'$ and $\tilde{A}\,^1A''$ states of HPO and DPO, obtained from rotational analyses of LIF, emission and/or microwave spectra of Refs. 1, 2, and 6, respectively, and from the *ab initio* PEFs computed in the present study (the expectation values, $\langle r \rangle$, of the vibrational wave function for the vibrational level with all vibrational quantum numbers equal to zero) are compared in Table V. Firstly, best *ab initio* r_0 geometrical parameters have been estimated based on the best estimated r_e geometrical parameters and the differences between the computed r_e and r_0 geometrical parameters obtained from the PEFs/anharmonic vibrational wave functions (see Tables II and IV). In addition, the best *ab initio* r_0 rotational constants have been computed using the best *ab initio* r_0 geometrical parameters, and the associated uncertainties have been estimated by taking the differences between the best *ab initio* values and those computed from the respective PEFs. It can be seen that the estimated uncertainties associated with the best theoretical A_0 values are significantly larger than those associated with the other two r_0 rotational constants, B_0 and C_0, for both states of HPO and DPO. In fact, it can be seen from Table V that the spread of available A_0 values, whether obtained experimentally and/or computationally, is significantly larger than those of B_0 and C_0. For example, the A_0 values of the $\tilde{X}\,^1A'$ and $\tilde{A}\,^1A''$ states of HPO of 8.670 and 7.990 cm^{-1}, respectively, computed based on r_0 geometrical parameters reported from the LIF/emission study of Ref. 1 are smaller than those reported from emission [8.8511(18) and 8.2689(9) cm^{-1}] and microwave [8.838 37(46) cm^{-1}] studies of Refs. 2 and 6, respectively, by over 0.16 cm^{-1}, while for the other two r_0 rotational constants, the differences are less than 0.005 cm^{-1}. All the above considerations show significantly larger uncertainties in A_0 than in B_0 and C_0, whether obtained experimentally or computationally.

Secondly, in converting geometrical parameters to rotational constants, it was found that, with bond lengths to three decimal places in angstroms and a bond angle to one decimal place in degrees, the corresponding rotational constants are at best reliable to three decimal places in cm^{-1}. This is the case for converting both *ab initio* and also experimentally derived geometrical parameters to rotational constants. For instance, the r_0 rotational constants computed employing the r_0 geometrical parameters of the $\tilde{X}\,^1A'$ state of HPO reported in Ref. 6 differ from the r_0 rotational constants obtained from rotational analysis of the microwave spectrum reported also in Ref. 6 in the third decimal place for all three rotational constants (see Table V). It should also be noted that, in Ref. 2, in order to obtain the r_0 structures of the $\tilde{X}\,^1A'$ and $\tilde{A}\,^1A''$ states of HPO, geometrical parameters were arbitrarily chosen to give rotational constants which agreed with experimental ones to within 0.002 cm^{-1}. All the above considerations imply that in converting geometrical parameters to rotational constants and vice versa, the accuracies are probably at the third decimal place for rotational constants in cm^{-1}, and at the third and first decimal places for bond length and angle in angstroms and degrees, respectively, for this type of molecule.

Thirdly, we focus on the r_0 bond angles of the $\tilde{A}\,^1A''$ state of HPO and DPO because the r_e bond angle of the $\tilde{A}\,^1A''$ state of HPO is a main issue to be resolved in the present study and the r_e geometry is usually derived from the r_0 geometry by including some form of anharmonic correction (for example, the r_e bond lengths of the $\tilde{X}\,^1A'$ state of HPO were obtained assuming anharmonic constants of the corresponding diatomics in Ref. 6). When all available r_0 bond angles, as shown in Table V, are considered, one striking observation is that, although the r_0 bond angle of 105° of the $\tilde{A}\,^1A''$ state of HPO derived from r_0 rotational constants obtained from the emission spectrum of Ref. 2 is significantly larger than the values obtained from other sources (less than 98°), the rotational constants, particularly B_0 and C_0, from Ref. 2 are not very different from available values obtained from other sources. Of course, it has been concluded in Ref. 1 that the excited state r_0 structure of HPO derived from the emission study of Ref. 2 is substantially in error. It appears that the r_0 rotational constants reported in Ref. 2 are reasonably reliable. However, for this type of C_S molecule, the r_0 geometrical parameters derived from the rotational constants are not unique and depend on the initial estimates used in the fitting.

Lastly, if we compare the estimated best *ab initio* r_0 rotational constants of the $\tilde{A}\,^1A''$ state of HPO and DPO with available experimental values, the agreement of within 0.004 cm^{-1} for B_0 and C_0 values is very good. Although the discrepancies in A_0 values between theory and experiment are larger (the largest being approximately 0.15 cm^{-1}), they are neither considerably larger than the estimated theoretical uncertainties (approximately 0.06 cm^{-1}) nor larger than the difference between different experimentally derived A_0 values [e.g., 8.2689 cm^{-1} from Ref. 2 and 7.990 cm^{-1} from Ref. 1 (computed from r_0 geometry)]. In fact, the best *ab initio* A_0 value for the $\tilde{A}\,^1A''$ state of HPO is in between the two experimentally derived values of Refs. 1 and 2. In view of the above comparisons, it is concluded that the best *ab initio* r_0 rotational constants of the $\tilde{A}\,^1A''$ state of HPO and DPO agree reasonably well with available experimentally derived values. In this connection, it can be concluded that the best *ab initio* r_e geometry of the $\tilde{A}\,^1A''$ state of HPO obtained from the present study is not inconsistent with available experimentally derived r_0 rotational constants, although the $\tilde{A}\,^1A''$ state bond angle of Ref. 2 of 105° is clearly too large, with the smaller value of Ref. 1 of 97.69° being favored (the recommended computed *ab initio* value is 94.5°).

IV. CONCLUDING REMARKS

State-of-the-art *ab initio* calculations have been carried out on the $\tilde{X}\,^1A'$ and $\tilde{A}\,^1A''$ states of HPO. Firstly, it is pleasing to conclude that the best *ab initio* T_c/T_0 values for the $\tilde{A}\,^1A''$ state of HPO/DPO agree with available experimental values to within 0.04 eV. This is a significant improvement from previous *ab initio* studies.[1,4] Secondly, the best *ab initio* equilibrium geometry of the $\tilde{A}\,^1A''$ state of HPO has a bond angle of 94.5°, which includes basis set extension to the CBS

limit and core correlation effects. A theoretical uncertainty of ±0.4° is estimated for this bond angle based on MRCI+D values obtained using different basis sets in the present study. In addition, based on the comparison between RCCSD(T) and MRCI+D results for the $\tilde{X}\,^1A'$ state of HPO, the estimated best MRCI+D bond angle is expected to have an uncertainty of 0.1°. All these considerations lead to the conclusion that the best equilibrium bond angle of the $\tilde{A}\,^1A''$ state of HPO obtainable from *ab initio* calculations should be 94.5±0.3°.

We have also simulated the $\tilde{A}\,^1A''(0,0,0)-\tilde{X}\,^1A'$ SVL emission spectra of HPO and DPO using a method which includes allowance for Duschinsky rotation and anharmonicity. In these spectral simulations, both the best *ab initio* equilibrium geometries and experimentally derived geometries of the two electronic states involved have been employed. It has been found that the simulated spectra employing the best *ab initio* geometries match the corresponding observed spectra better than those employing experimentally derived geometries. Although we have not derived an upper state geometry through IFCA by fixing the lower state geometry to an experimentally derived geometry and varying the upper state geometry systematically, and carrying out FC factor calculations for each upper and lower state geometries, the excellent match between simulated spectra employing the best *ab initio* geometries of both states and the experimental spectra supports the conclusion that the best *ab initio* geometries of both states are already highly reliable. In this connection, it is concluded that the best *ab initio* bond angle of the $\tilde{A}\,^1A''$ state of HPO of 94.5° is currently the most reliable value.

Finally, it should be noted that, deriving geometrical information on an electronic state for a C_S molecule such as HPO by comparing simulated electronic spectra, obtained from computed FC factors, with observed spectra, is similar to deriving geometrical parameters from rotational analysis of a high-resolution spectrum. Both require some kind of "matching" (or fitting) between computed and experimentally measured data. However, in the case of employing FC factors in the spectral simulation, and particularly with the IFCA procedure, the equilibrium geometries, and not the r_0 geometries, of the two states are used and/or derived. Rotational constants and r_0 geometries are not involved, as equilibrium geometrical parameters are used and/or derived directly, without the need of conversion from r_0 structure or rotational constants. Of course, in the case of using IFCA to compute the vibrational structure of an electronic spectrum, the information of the r_e and r_0 structures of the two electronic states involved in the electronic transition is embedded in the *ab initio* PEFs, which are used to compute anharmonic vibrational wave functions and FC factors of the two electronic states involved. Providing that the *ab initio* PEFs employed are reliable and the equilibrium geometry of one state involved is reliably known, applying IFCA to compute the vibrational structure of an electronic spectrum is a reliable and direct way to derive equilibrium geometrical parameters of the other state.

ACKNOWLEDGMENTS

Financial support from the Research Grant Council (RGC) of the Hong Kong Special Administrative Region (HKSAR, Grant Nos. PolyU 5003/04P and PolyU 5014/06P) is acknowledged for this work. The authors are also grateful to the provision of computational resources from the EPSRC (UK) National Service for Computational Chemistry Software.

[1] B. S. Tackett and D. J. Clouthier, J. Chem. Phys. **117**, 10604 (2002).
[2] M. Larzilliere, N. Damany, and Lam T. My, Chem. Phys. **46**, 401 (1980).
[3] G. Herzberg, *Molecular Spectra and Molecular Structure III. Electronic Structure of Polyatomic Molecules* (van Nostrand, Toronto, 1967).
[4] A. Luna, M. Merchan, and B. O. Roos, Chem. Phys. **196**, 437 (1995).
[5] J. S. Francisco, Chem. Phys. **287**, 303 (2003).
[6] H. Ozeki and S. Saito, J. Mol. Spectrosc. **219**, 305 (2003).
[7] F.-T. Chau, J. M. Dyke, E. P. F. Lee, and D. K. W. Mok, J. Chem. Phys. **115**, 5816 (2001).
[8] F. T. Chau, J. M. Dyke, E. P. F. Lee, and D. K. W. Mok, J. Chem. Phys. **118**, 4025 (2003).
[9] C. Hampel, K. Peterson, and H.-J. Werner, Chem. Phys. Lett. **190**, 1 (1992).
[10] J. D. Watts, J. Gauss, and R. J. Bartlett, J. Chem. Phys. **98**, 8718 (1993).
[11] H.-J. Werner and P. J. Knowles, J. Chem. Phys. **82**, 5053 (1985).
[12] H.-J. Werner and P. J. Knowles, J. Chem. Phys. **89**, 5803 (1988).
[13] D. E. Woon and T. H. Dunning, Jr., J. Chem. Phys. **98**, 1358 (1993).
[14] T. H. Dunning, Jr., K. A. Peterson, and A. K. Wilson, J. Chem. Phys. **114**, 9244 (2001).
[15] K. A. Peterson and T. H. Dunning, Jr., J. Chem. Phys. **117**, 10548 (2002).
[16] E. P. F. Lee, J. M. Dyke, F.-T. Chau, and W.-K. Chow, Chem. Phys. Lett. **376**, 465 (2003).
[17] A. Halkier, T. Helgaker, W. Klopper, P. Jorgensen, and A. G. Csaszar, Chem. Phys. Lett. **310**, 385 (1999).
[18] S. Carter and N. C. Handy, J. Chem. Phys. **87**, 4294 (1987).
[19] H.-J. Werner, P. J. Knowles, J. Almlöf, R. D. Amos, A. Berning, D. L. Cooper, M. J. O. Deegan, A. J. Dobbyn, F. Eckert, S. T. Elbert, C. Hampel, R. Lindh, A. W. Lloyd, W. Meyer, A. Nicklass, K. Peterson, R. Pitzer, A. J. Stone, P. R. Taylor, M. E. Mura, P. Pulay, M. Schütz, H. Stoll, and T. Thorsteinsson, MOLPRO, a package of *ab initio* programs.
[20] J. K. G. Watson, Mol. Phys. **15**, 479 (1968).
[21] J. K. G. Watson, Mol. Phys. **19**, 465 (1970).
[22] C. Puzzarini, J. Mol. Struct. **780–781**, 238 (2006).
[23] M.-L. Liu, C.-L. Lee, A. Bezant, G. Tarczay, R. J. Clark, T. A. Miller, and B.-C. Chang, Phys. Chem. Chem. Phys. **5**, 1352 (2003).
[24] M. Larzilliere and M. E. Jacox, J. Mol. Spectrosc. **79**, 132 (1980).